IOPscience iopscience.iop.org

Home Search Collections Journals About Contact us My IOPscience

Controlling single-photon transport properties in a waveguide coupled with two separated atoms

This article has been downloaded from IOPscience. Please scroll down to see the full text article.

2013 J. Phys. B: At. Mol. Opt. Phys. 46 145504

(http://iopscience.iop.org/0953-4075/46/14/145504)

View the table of contents for this issue, or go to the journal homepage for more

Download details:
IP Address: 112.65.124.195
The article was downloaded on 12/08/2013 at 03:17

Please note that terms and conditions apply.

J. Phys. B: At. Mol. Opt. Phys. **46** (2013) 145504 (6pp) doi:10.1088/0953-4075/46/14/145504

Controlling single-photon transport properties in a waveguide coupled with two separated atoms

Xiao Fei Zang[1], Tao Zhou[2], Bin Cai[1] and Yi Ming Zhu[1]

[1] Shanghai Key Lab of Modern Optical System and Engineering Research Center of Optical Instrument and System, Ministry of Education, University of Shanghai for Science and Technology, No. 516 JunGong Road, Shanghai 200093, People's Republic of China
[2] School of Mathematics and Physics, Shanghai University of Electric Power, No, 2103 PingLiang Road, Shanghai 200090, People's Republic of China

E-mail: ymzhu@usst.edu.cn

Received 16 December 2012, in final form 3 April 2013
Published 26 June 2013
Online at stacks.iop.org/JPhysB/46/145504

Abstract
Based on the symmetric, asymmetric atom–photon couplings and the phase difference between two separated atoms, single-photon transport properties in an optical waveguide coupled with two separated two-level atoms are theoretically investigated. The transmission and reflection amplitudes for the single-photon propagation in such a hybrid system are deduced via a real-space approach. Several new phenomena such as phase-coupled induced transparency, single-photon switches, symmetric and asymmetric bifrequency photon attenuators are analyzed. In addition, the dissipation effect of such a hybrid system is also discussed.

(Some figures may appear in colour only in the online journal)

1. Introduction

In the past few years, controlling single-photon transport properties in cavity quantum electrodynamics (CQED) systems embedded with an atom or a quantum dot (QD) has attracted much attention, due to its potential applications in all-optical quantum information processing, optical quantum computing, etc [1–24]. As a typical system, a one-dimensional optical waveguide coupled with a two-level atom (TLA) has been applied to manipulate a single-photon transmission spectrum [25, 26]. In such a linear hybrid system, the incident single-photon is completely reflected when on-resonant with the transition frequency of the TLA, while the incident single photon is completely transmitted when far-detuning (off-resonant) from the atom transition frequency. In contrast to the above linear one-dimensional waveguide–atom hybrid system, Zhou *et al* proposed a nonlinear one-dimensional coupled-resonator waveguide embedded with a TLA in one cavity to study the coherent single-photon transport properties [27]. Their results demonstrated that the transmission and reflection spectrum were beyond the usual Breit–Wigner and Fano line shapes due to the nonlinear dispersion relation arising from tight-binding intercavity couplings. Furthermore, asymmetric atom–photon coupling was also proposed to control the single-photon transmission spectrum [28], where the single-photon transmission spectrum was well controlled by using asymmetric atom–photon couplings, and an all-optical single-frequency attenuator was also realized by control of the asymmetric atom–photon coupling.

Recently, much attention has been focused on the single-photon transmission spectrum in the system of a waveguide coupled with two (or more) separated atoms (or QDs) [29–34]. In such a multi-atom (or multi-QDs) system, many new phenomena such as Fano-like lineshape and electromagnetically induced transparency-like (EIT-like) lineshape transmission spectrums have been found by tuning the distance between these atoms. Most of the above studies of the single-photon transmission spectrum in a multi-atom system are just focused on the symmetric couplings between the incident single photon and the TLAs (or QDs); however, single-photon transport properties in such a multi-atom system under asymmetric atom–photon couplings have not been fully studied, which may lead to new physics on the coherent transport of the single photon. In this paper, motivated

 © 2013 IOP Publishing Ltd Printed in the UK & the USA

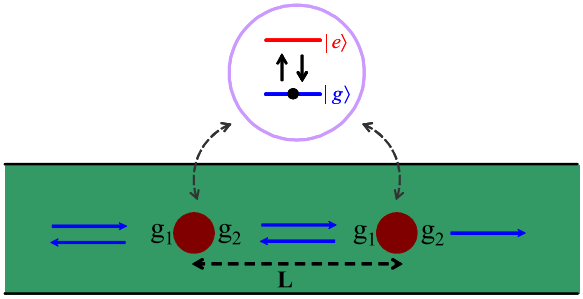

Figure 1. Schematic of the hybrid optical system composed of an optical waveguide coupled with two separated TLAs.

by the symmetric and especially the asymmetric atom–photon couplings, the single-photon transmission properties in an optical waveguide coupled with two separated atoms are investigated in detail. Many new physical phenomena such as phase-coupled induced transparency, single-photon switches and symmetric and asymmetric bifrequency photon attenuators are realized by controlling the symmetric and asymmetric atom–photon couplings and the phase difference induced by these two separated atoms.

2. Theoretical model

Figure 1 depicts a hybrid system composed of an optical waveguide embedded with two separated TLAs (the distance between these two separated atoms is L). By using the linearization of photonic dispersion with a waveguide mode, the effective Hamiltonian of the interaction between the propagating photons and optical waveguide coupled with just one TLA under the asymmetric atom–photon coupling can be written as

$$\begin{aligned} H_{\rm eff} = \frac{H}{\hbar} = {\rm i}v_g\Big\{ & \int {\rm d}x C_L^+(x)\frac{\partial}{\partial x}C_L(x) - C_R^+(x)\frac{\partial}{\partial x}C_R(x) \\ & + g_1\delta(x)[C_L^+(x)a_g^+a_e + C_L(x)a_e^+a_g] \\ & + g_2\delta(x)[C_R^+(x)a_g^+a_e + C_R(x)a_e^+a_g]\Big\} + \Omega a_e^+a_e, \end{aligned} \tag{1}$$

where v_g is the group velocity of the single photon; $C_R^+(C_R)$, $C_L^+(C_L)$ are the bosonic creation (annihilation) operators of the right- and left-moving photons, respectively; $a_g(a_g^+)$ and $a_e(a_e^+)$ are the creation (annihilation) operators of the ground and excited states of the TLA; and $\Omega(\Omega = \omega_e - \omega_g)$ is the transition frequency of the TLA. The atom–photon couplings can be written as $g_{1,2} = [2\pi\hbar/\omega_{p1(p2)}]^{1/2}\Omega D \cdot E_{p1(p2)}$, where D is the dipole moment of the TLA; ω_{p1}, E_{p1} and ω_{p2}, E_{p2} are the frequency, polarization of the left- and right-travelling photons, respectively.

The scattering eigenstate of equation (1) can be expressed as

$$|E_k\rangle = \int {\rm d}x[\phi_R(x)C_R^+(x) + \phi_L(x)C_L^+(x)]|0,g\rangle + f_e|0,e\rangle, \tag{2}$$

where $|0,i\rangle$ $(i = g, e)$ represents a non-photon in the optical waveguide and the corresponding state $|i\rangle$ of TLA and f_e is the excitation state amplitude of the state $|e\rangle$.

By solving the eigenvalue equation of $H|E_k\rangle = E_k|E_k\rangle$, single-photon transmission and reflection coefficients are written as [28]

$$\begin{cases} t = \dfrac{g_1^2 - g_2^2 + 2{\rm i}v_g(\Omega-\omega)}{g_1^2 + g_2^2 + 2{\rm i}v_g(\Omega-\omega)} \\ r = \dfrac{-2g_1g_2}{g_1^2 + g_2^2 + 2{\rm i}v_g(\Omega-\omega)} \end{cases}, \tag{3}$$

where $\omega = E_k/\hbar$.

According to [26, 36, 37], the transfer matrix for equation (3) (one atom embedded in an optical waveguide) has the following form:

$$\begin{pmatrix} a' \\ b' \end{pmatrix} = \begin{bmatrix} \dfrac{t^2 - r^2}{t} & \dfrac{r}{t} \\ -\dfrac{r}{t} & \dfrac{1}{t} \end{bmatrix} \begin{pmatrix} a \\ b \end{pmatrix}, \tag{4}$$

where a and b are, respectively, the incoming and outgoing wave amplitudes on the left side of the atom; and a' and b' are the outgoing and incoming wave amplitude on the right side of the atom, when the single photon comes from the left side. Therefore, these wave amplitudes can be written as $a = 1$, $b = r$, $a' = t$, $b' = 0$ [36].

So, when the optical waveguide is coupled with two separated atoms, as shown in figure 1, the transfer matrix of such a multi-atom system can be described as [26, 36, 37]

$$\begin{pmatrix} a''' \\ b''' \end{pmatrix} = M \begin{pmatrix} a \\ b \end{pmatrix}, \tag{5}$$

where $M = \begin{bmatrix} \frac{(t_2^2 - r_2^2)}{t_2} & \frac{r_2}{t_2} \\ -\frac{r_2}{t_2} & \frac{1}{t_2} \end{bmatrix} \begin{bmatrix} {\rm e}^{{\rm i}\theta} & 0 \\ 0 & {\rm e}^{-{\rm i}\theta} \end{bmatrix} \begin{bmatrix} \frac{(t_1^2 - r_1^2)}{t_1} & \frac{r_1}{t_1} \\ -\frac{r_1}{t_1} & \frac{1}{t_1} \end{bmatrix}$. Here a and b are, respectively, the incoming and outgoing wave amplitudes on the left side of the left atom; and a''' and b''' are the outgoing and incoming wave amplitudes on the right side of the right atom, the w single photon coming from the left side. Here, $\theta = \omega L/c$ is the phase difference between these two separated atoms. $t_1(t_2)$ and $r_1(r_2)$ are the corresponding transmission and reflection amplitudes of the left (right) atom, respectively. Therefore, the transmission amplitude t and transmission intensity T of the hybrid system of figure 1 is defined by [26, 36, 37]

$$\begin{cases} t = \dfrac{1}{M_{22}} = \dfrac{{\rm e}^{{\rm i}\theta}t_1t_2}{1 - r_1r_2\exp({\rm i}2\theta)} \\ T = |t|^2 = \left|\dfrac{{\rm e}^{{\rm i}\theta}t_1t_2}{1 - r_1r_2\exp({\rm i}2\theta)}\right|^2 = \left|\dfrac{t_1t_2}{1 - r_1r_2\exp({\rm i}2\theta)}\right|^2 \end{cases}. \tag{6}$$

From equations (3)–(6), we can find that the single-photon transport properties are determined by the parameters of g_1, g_2, θ, Ω_1 and Ω_2(here, Ω_1 and Ω_2 are the transition frequency of the left and right atoms, respectively).

3. Results and discussion

First, we investigate the single-photon transport properties with symmetric atom–photon couplings ($g_1 = g_2 = 0.2$) and $\Omega_1 = \Omega_2 = \Omega$, as shown in figure 2.

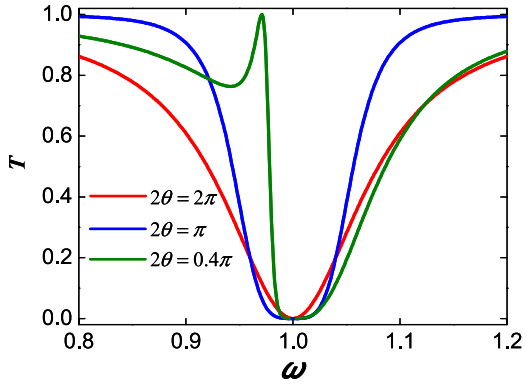

Figure 2. The single-photon transmission spectrum under the symmetrical atom–photon couplings ($g_1 = g_2 = 0.2$). $2\theta = 2\pi$ for the red line, $2\theta = \pi$ for the blue line, and $2\theta = 0.4\pi$ for the green line. The coupling strengths g_1 and g_2 are in units of V_g.

When $2\theta = 2\pi$, a symmetrical Lorentz line shape of the single-photon transmission spectrum is depicted by the red line in figure 2. The dip in the transmission spectrum at $\omega = \Omega$ can be explained by the fact that the incident photon is on-resonant with the transition frequency of the TLA. In this case, the left TLA is excited while the right TLA is not excited. Therefore, the incident single photon from the left side is completely reflected by the left atom, leading to a dip at $\omega = \Omega$. In the case of $2\theta = \pi$, a symmetrical line shape of the transmission spectrum is shown by the blue line in figure 2. Here, the transmission is the sum of two new resonances of $t_2' = [(1+i)^2A]/[i(\omega - \Omega - A) - A]$ and $t_2' = [(1-i)^2A]/[i(\omega - \Omega + A) - A]$, where $A = g^2/v_g$ (the transmission intensity T of the hybrid system in figure 1 is defined as $T = \left|1 + e^{-i\theta}(t_1' - t_2')/2\right|^2$ and both of the atom–photon couplings for the new resonance are still g [34]). When $2\theta \neq n\pi$ (n is an integer), the resonance frequencies can be considered as $\Omega_1' = \Omega + A\sin\theta$ and $\Omega_2' = \Omega - A\sin\theta$, respectively. Therefore, the transmission spectrum of the incident single photon is modified by the phase difference of θ and an asymmetric Fano-type line shape of the transmission spectrum can be obtained, as shown in figure 2 (green line).

Now, we study coherent transport properties of the single photon under asymmetric atom–photon couplings, where $g_1 \neq g_2$ and $\Omega_1 = \Omega_2 = \Omega$. Figure 3(a) shows the single-photon transmission spectrum with asymmetrical atom–photon couplings and $2\theta = 2\pi$. There is one peak at $\omega = \Omega$ and two side dips in the transmission spectrum, which would not occur in the situation of the symmetric atom–photon when the two atoms are in tune ($\Omega_1 = \Omega_2 = \Omega$). Here, the peak at $\omega = \Omega$ is induced by the asymmetric atom–photon couplings of $g_1 \neq g_2$ and the phase difference (θ) caused by these two separate atoms. When the incident single photon is on-resonant with the TLA, it will be completely reflected for the symmetric atom–photon couplings $g_1 = g_2$; however, for the asymmetric atom–photon couplings, the single photon can partially transmit through the on-resonance TLA due to the redistribution of energy and momentum of the incident photon after scattering by the atom [28]. In this case, these two TLAs (even though on-resonance) can be considered as a partially reflecting/transmitting mirror. Therefore, the peak at $\omega = \Omega$ is well understood as follows: these two atoms and the optical waveguide can be considered as a Fabry–Pérot resonator. Although the atoms are on-resonant with the incident photon, the single photon can also partially pass through the left atom. So, the forward and backward light fields between these two separated atoms interfere with each other. In addition, the interference is modulated by the phase difference depending on the distance between these two atoms and resulting in single-photon responses at different incident frequency. Here, the peak at $\omega = \Omega$ is caused by the constructive interference of light fields due to the phase difference (θ) between these two separated atoms. So, the phenomenon in figure 3(a) (EIT-like transmission spectrum) can be defined as the phase-coupled induced transparency as discussed in [35]. With increasing the ratio of g_1/g_2, the transmittance values of these two-side peaks (Rabi splittings) can be changed from 0 to 1, which can be considered as a symmetric bifrequency-like photon attenuator. When $2\theta = \pi$, the single-photon transmission spectrum is different from that of $2\theta = 2\pi$. Only one dip appears at $\omega = \Omega$, as shown in figure 3(b), which is caused by the destructive interference between the forward and backward light fields. By increasing the ratio of g_1/g_2, the incident photon with frequency of $\omega = \Omega$ can be controlled from 0 to 1, which means that a single-frequency of the photon attenuator can be realized by manipulating the asymmetric atom–photon couplings. Comparing the transmission spectrum in figures 3(a), (b) and 2 (red line), we can find that two kinds of optical switches can be obtained by controlling the symmetric and asymmetric atom–photon couplings and also the phase difference between these two atoms. For example, when $2\theta = 2\pi$ and $g_1 = g_2$, the single transmission spectrum shows a dip (with $T = 0$) at $\omega = \Omega$ (the red line $g_1 = g_2 = 0.2$ of figure 3(c)), while it shows a peak (with $T = 1$) at $\omega = \Omega$ for the asymmetrical atom–photon couplings (the green line $g_1 = 0.2$, $g_2 = 0.15$ of figure 3(c)). That is to say, a single-photon switch can be realized by changing the atom–photon couplings. Furthermore, for the asymmetric atom–photon couplings, another kind of single-photon switch at $\omega = \Omega$ can also be achieved by controlling the phase difference between these two atoms, as shown in figure 3(c) (blue line for $2\theta = \pi$, green line for $2\theta = 2\pi$). For $2\theta \neq n\pi$ (n is an integer) such as $2\theta = 0.4\pi$ and asymmetric atom–photon couplings, Fano-type line shapes of the transmission spectrum also appears (figure 3(d)), which is similar to the case of the symmetric atom–photon couplings case shown in figure 2 (green line). By manipulating the ratio of g_1/g_2, the dip near $\omega = \Omega$ can also be changed from 0 to 1, totally resulting from the asymmetric atom–photon couplings.

In addition, we also discuss the single-photon transport properties under asymmetric atom–photon couplings, when the left atom is detuned from the right atom. Figure 4(a) depicts the single-photon transmission spectrum for the case of $2\theta = 2\pi$ and $\Omega_1 = 0.9\ \Omega$ (for the left atom), $\Omega_2 = 1.1\ \Omega$ (for the right atom). For $g_2 = 0.15$, a EIT-like transmission spectrum structure is shown by the red line in figure 4(a). Two side dips with $T = 0$ located at $\omega = \Omega_1, \Omega_2$, and the complete transmission peak with $T = 1$ located at $\omega = (\Omega_1 + \Omega_2)/2$. In other words, these two separated atoms behave as two mirrors

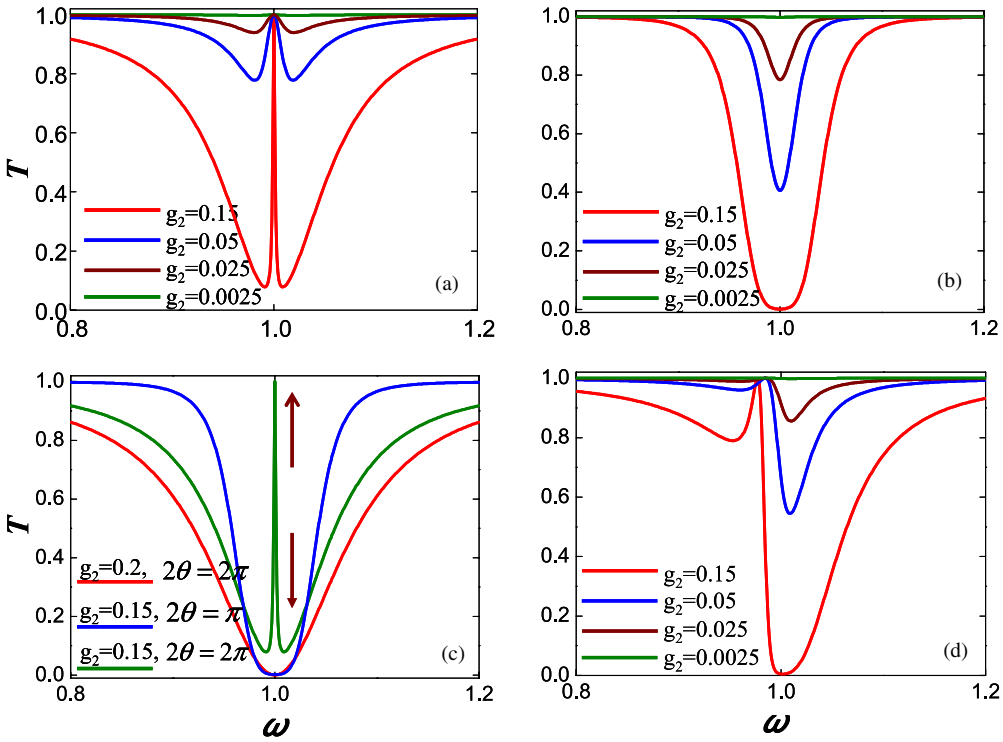

Figure 3. The single-photon transmission spectrum under asymmetrical atom–photon couplings ($g_1 \neq g_2$ and $g_1 = 0.2$) and $2\theta = 2\pi$ (a), $2\theta = \pi$ (b), $2\theta = 0.4\pi$ (d). (c) Single-photon switch by controlling the atom–photon couplings and the phase difference between these two separated atoms. The coupling strengths g_1 and g_2 are in units of V_g.

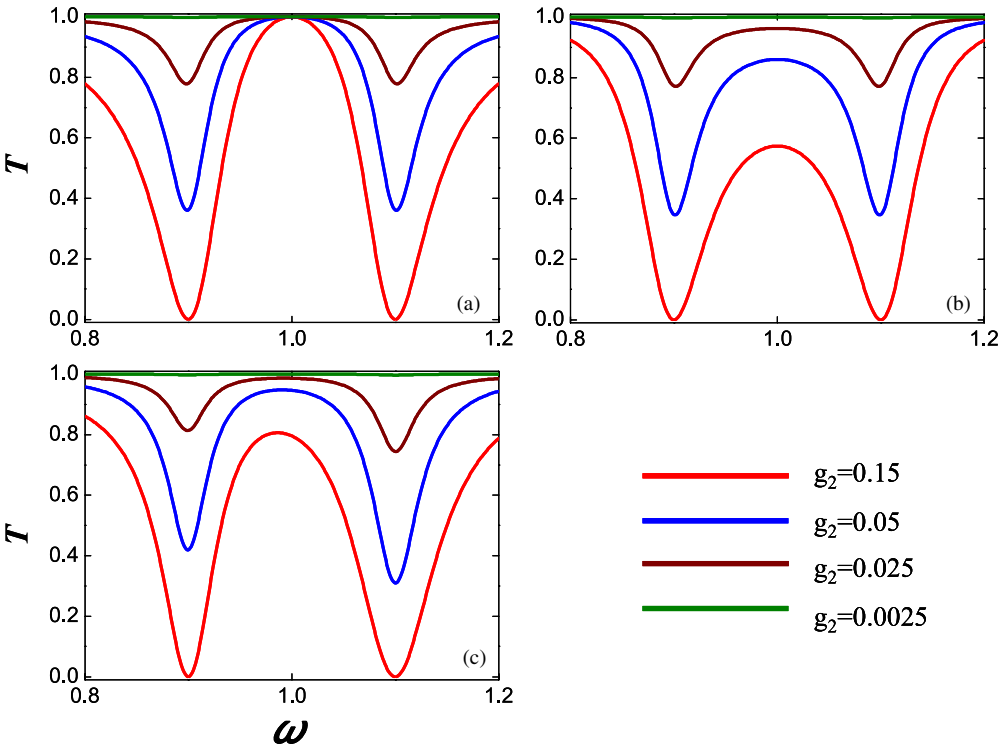

Figure 4. The single-photon transmission spectrum under symmetrical atom–photon couplings and $2\theta = 2\pi$ (a), $2\theta = \pi$ (b), $2\theta = 0.4\pi$ (c) with $\Omega_1 = 0.9\ \Omega$ (left atom) and $\Omega_2 = 1.1\ \Omega$ (right atom) and $\Omega = 1.0$. (d) The energy-level configuration of the Λ-type three-level atom. $V_1 = {g_1}^2/2\ v_g = 0.2$ and $V_2 = {g_2}^2/2\ v_g$. The coupling strengths g_1 and g_2 are in units of V_g.

with two different resonance frequencies (corresponding to two side dips). With the increasing of the g_1/g_2 ratio, the transmittivity of these two-side peaks at $\omega = \Omega_1, \Omega_2$ can be changed from 0 to 1, leading to a symmetric bifrequency photon attenuator. For $2\theta = \pi$, there is still the EIT-like transmission spectrum structure for the incident single photon.

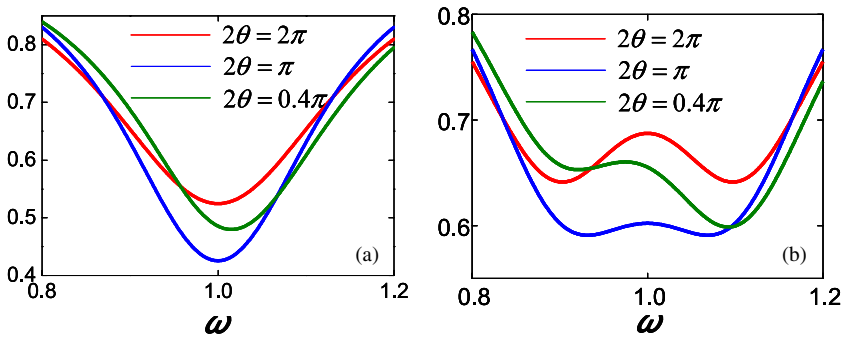

Figure 5. The single-photon transmission spectrum under asymmetrical atom–photon couplings ($g_1 = 0.2$, $g_2 = 0.15$) and atom dissipation ($1/T_a = 0.1\ \Omega$): (a) $\Omega_1 = \Omega_2 = \Omega$, $2\theta = 2\pi$ (red line), $2\theta = \pi$ (blue line), $2\theta = 0.4\pi$ (green line); (b) $\Omega_1 = \Omega_2 = \Omega$, $2\theta = 2\pi$ (red line), $2\theta = \pi$ (blue line), $2\theta = 0.4\pi$ (green line). The coupling strengths g_1 and g_2 are in units of V_g.

But, the peak located at $\omega = (\Omega_1 + \Omega_2)/2$ no longer has $T = 1$ for $V_2 = 0.15$. Here, it can also be explained that the forward and backward light fields interfere with each other and meanwhile the peak at $\omega = (\Omega_1 + \Omega_2)/2$ with $T \neq 1$ is also caused by the destructive interference of the light fields between these two separated atoms. By controlling the asymmetric atom–photon couplings, a symmetric bifrequency photon attenuator can also be realized for $2\theta = \pi$. When $2\theta \neq n\pi$ (n is an integer) such as $2\theta = 0.4\pi$, the transmission spectrum is different from that of $2\theta = n\pi$. For example, when $g_2 = 0.15$ and $2\theta = 0.4\pi$ (red line in figure 4(c)), there is an asymmetric EIT-like transmission spectrum structure due to the phase (θ) modulation. So, when we tune the ratio of g_1/g_2, asymmetric transmittance at $\omega = \Omega_1, \Omega_2$ will occur, which can be considered as an asymmetric bifrequency photon attenuator. In other words, all of the EIT-like transmission spectrum in these three cases ($2\theta = 2\pi, \pi, 0.4\pi$) can also be mapped into the phase-coupled induced transparency as described in [35]. At $\omega = (\Omega_1+\Omega_2)/2$, both of these two atoms can also be considered as two partially reflecting/transmitting mirrors. The waveguide region between the atoms acts as a Fabry–Pérot cavity bounded by these two partially reflecting mirrors. The cavity is resonant at $\omega = (\Omega_1 + \Omega_2)/2$, and displays a transmission maximum, leading to the EIT-like transmission spectrum. In addition, the peak at $\omega = (\Omega_1 + \Omega_2)/2$ is also modulated by the phase difference between these two separated atoms. These two dips at $\omega = \Omega_1, \Omega_2$ are corresponding to Rabi splitting, which can be controlled by asymmetric atom–photon couplings. Therefore, the transmission probability of the resonant incident photons at $\omega = (\Omega_1 + \Omega_2)/2$ can also be changed from 1 to 0, resulting in symmetric and asymmetric bifrequency photon attenuators.

Finally, we investigate the realistic physical model of our hybrid system by considering the dissipation effect of the atom as discussed in [12]. When $\Omega_1 = \Omega_2 = \Omega$ and $g_1 = 0.2$, $g_2 = 0.15$, figure 5(a) depicts the single-photon transmission spectrum with atom dissipation $1/T_a = 0.1\ \Omega$ under asymmetric atom–photon couplings. In this case, there is a dip at $\omega = \Omega$. The EIT-like and Fano-type transmission spectrum (in the non-dissipation case) disappears due to the effect of atom dissipation. In addition, the dip at $\omega = \Omega$ cannot be tuned from 0 to 1 by using the asymmetric atom–photon couplings (not shown in figure 5). Therefore, in the realistic case, we can just achieve an imperfect single-frequency photon attenuator by controlling the asymmetric atom–photon coupling, when $\Omega_1 = \Omega_2 = \Omega$. When $\Omega_1 = 0.9\ \Omega$ (for the left atom), $\Omega_2 = 1.1\ \Omega$ (for the right atom), symmetric and asymmetric EIT-like transmission spectra also appear, as shown in figure 5(b). In this situation, the transmission spectra are very similar to that of the non-dissipation case (shown in figure 4). However, at $\omega = \Omega$, the incident single photon cannot be fully transported through the hybrid system ($T \neq 1$ at $\omega = \Omega$ due to the atom dissipation), leading to the imperfect EIT-like transmission spectrum due to the atom dissipation. Furthermore, the corresponding Rabi splitting at $\omega = 0.9\ \Omega$ and $\omega = 1.1\ \Omega$ cannot be tuned from 0 to 1 by controlling the asymmetric atom–photon coupling, resulting in imperfect bifrequency photon attenuators (not shown in figure 5(b)).

4. Conclusion

In conclusion, we have theoretically investigated the coherent transport properties of the single photon in a hybrid system containing an optical waveguide coupled with two separated TLAs. By controlling the symmetric as well as asymmetric atom–photon couplings and the phase difference caused by the separated atoms, many interesting phenomena such as phase-coupled induced transparency, single-photon switches and symmetric and asymmetric single-frequency and bifrequency photon attenuators can be realized. Our results may be useful in manipulating light–matter interactions in CQED systems and may have potential applications in all-optical quantum information processing.

Acknowledgments

This work is partly supported by the Major National Development Project of Scientific Instrument and Equipment (2011YQ150021), the Key Scientific and Technological Project of Science and Technology Commission of Shanghai Municipality (11DZ1110800), National Natural Science Foundation of China (11174207, 61138001, 61007059, 61205094), the Leading Academic Discipline Project of

Shanghai Municipal Government (S30502) and the Key Project of the Shanghai Municipal Science and Technology Commission (12JC1407100).

References

[1] Wallraff A, Schuster D I, Blais A, Frunzio L, Huang R S, Majer J, Kumar S, Girvin S M and Schoelkopf R J 2004 *Nature* **431** 162
[2] Yoshie T, Scherer A, Hendrickson J, Khitrova G, Gibbs H M, Rupper G, Ell C, Shchekin O B and Deppe D G 2004 *Nature* **432** 200
[3] Birnbaum K M, Boca A, Miller R, Boozer A D, Northup T E and Kimble H J 2005 *Nature* **436** 87
[4] Srinivasan K and Painter O 2007 *Nature* **450** 862
[5] Dayan B, Parkins A S, Aoki T, Ostby E P, Vahala K J and Kimble H J 2008 *Science* **319** 1062
[6] Hughes S 2007 *Phys. Rev. Lett.* **98** 083603
[7] Shen J-T and Fan S 2007 *Phys. Rev. Lett.* **98** 153003
[8] Wei L F, Liu Y X, Sun C P and Nori F 2006 *Phys. Rev. Lett.* **97** 237201
[9] Roy D 2011 *Phys. Rev. Lett.* **106** 053601
[10] Kolchin P, Oulton R F and Zhang X 2011 *Phys. Rev. Lett.* **106** 113601
[11] Zhou L, Dong H, Liu Y X, Sun C P and Nori F 2008 *Phys. Rev.* A **78** 063827
[12] Shen J T and Fan S 2009 *Phys. Rev.* A **79** 023837
[13] An J H, Feng M and Oh C H 2009 *Phys. Rev.* A **79** 032303
[14] Shi T, Fan S and Sun C P 2011 *Phys. Rev.* A **84** 063803
[15] Witthaut D and Sorensen A S 2010 *New. J. Phys.* **12** 043052
[16] Kim N C, Li J B, Yang Z J, Hao Z H and Wang Q Q 2010 *Appl. Phys. Lett.* **97** 061110
[17] Tan L and Hai L 2012 *J. Phys B: At. Mol. Opt. Phys.* **45** 035504
[18] Roy D 2010 *Phys. Rev.* B **81** 155117
[19] Zang X and Jiang C 2010 *J. Phys B: At. Mol. Opt. Phys.* **43** 065505
[20] Zang X and Jiang C 2010 *J. Phys B: At. Mol. Opt. Phys.* **43** 215501
[21] Jiahua L and Yu R 2011 *Opt. Express* **19** 20991
[22] Chang D E, Sorensen A S, Demler E A and Lukin M D 2007 *Nat. Phys.* **3** 807
[23] Cheng M T, Luo Y Q, Wang P Z and Zhao G X 2010 *Appl. Phys. Lett.* **97** 191903
[24] Chen G Y, Lambert N, Chou C H, Chen Y N and Nori F 2011 *Phys. Rev.* B **84** 045310
[25] Shen J T and Fan S 2005 *Phys. Rev. Lett.* **95** 213001
[26] Shen J T and Fan S 2005 *Opt. Lett.* **30** 2001
[27] Zhou L, Gong Z R, Liu Y X, Sun C P and Nori F 2008 *Phys. Rev. Lett.* **101** 100501
[28] Yan C H, Wei L F, Jia W Z and Shen J T 2011 *Phys. Rev.* A **84** 045801
[29] Kim N-C, Li J B, Yang Z J, Hao Z H and Wang Q Q 2010 *Appl. Phys. Lett.* **97** 061110
[30] Chen W, Chen G Y and Chen Y N 2010 *Opt. Express* **18** 10360
[31] Chen W, Chen G Y and Chen Y N 2011 *Opt. Lett.* **36** 3602
[32] Cheng G Y, Lambert N, Chou C H, Chen Y N and Nori F 2011 *Phys. Rev.* B **84** 045310
[33] Cheng M T, Ma X S, Luo Y Q, Wang P Z and Zhao G X 2011 *Appl. Phys. Lett.* **99** 223509
[34] Cheng M T and Song Y Y 2012 *Opt. Lett.* **37** 978
[35] Kekatpure R, Barnard E, Cai W S and Brongersma M L 2010 *Phys. Rev. Lett.* **104** 243902
[36] Xu Y, Li Y, Lee K R and Yariv A 2000 *Phys. Rev.* E **62** 7389
[37] Fan S H 2002 *Appl. Phys. Lett.* **80** 908